

Conditional Logical Message Passing Transformer for Complex Query Answering

Chongzhi Zhang

cschongzhizhang@mail.scut.edu.cn
South China University of Technology
Guangzhou, China

Junhao Zheng

junhaozheng47@outlook.com
South China University of Technology
Guangzhou, China

Zhiping Peng

Guangdong University of Petrochemical Technology
Maoming, China
Jiangmen Polytechnic
Jiangmen, China

Qianli Ma*

qianlima@scut.edu.cn
South China University of Technology
Guangzhou, China

ABSTRACT

Complex Query Answering (CQA) over Knowledge Graphs (KGs) is a challenging task. Given that KGs are usually incomplete, neural models are proposed to solve CQA by performing multi-hop logical reasoning. However, most of them cannot perform well on both one-hop and multi-hop queries simultaneously. Recent work proposes a logical message passing mechanism based on the pre-trained neural link predictors. While effective on both one-hop and multi-hop queries, it ignores the difference between the constant and variable nodes in a query graph. In addition, during the node embedding update stage, this mechanism cannot dynamically measure the importance of different messages, and whether it can capture the implicit logical dependencies related to a node and received messages remains unclear. In this paper, we propose Conditional Logical Message Passing Transformer (CLMPT), which considers the difference between constants and variables in the case of using pre-trained neural link predictors and performs message passing conditionally on the node type. We empirically verified that this approach can reduce computational costs without affecting performance. Furthermore, CLMPT uses the transformer to aggregate received messages and update the corresponding node embedding. Through the self-attention mechanism, CLMPT can assign adaptive weights to elements in an input set consisting of received messages and the corresponding node and explicitly model logical dependencies between various elements. Experimental results show that CLMPT is a new state-of-the-art neural CQA model.

*Corresponding author

Permission to make digital or hard copies of all or part of this work for personal or classroom use is granted without fee provided that copies are not made or distributed for profit or commercial advantage and that copies bear this notice and the full citation on the first page. Copyrights for components of this work owned by others than ACM must be honored. Abstracting with credit is permitted. To copy otherwise, or republish, to post on servers or to redistribute to lists, requires prior specific permission and/or a fee. Request permissions from [permissions@acm.org](https://permissions.acm.org).

Conference acronym 'XX, June 03–05, 2018, Woodstock, NY

© 2018 ACM.

ACM ISBN 978-1-4503-XXXX-X/18/06

<https://doi.org/XXXXXXXX.XXXXXXX>

CCS CONCEPTS

• **Computing methodologies** → Reasoning about belief and knowledge; Knowledge representation and reasoning; • **Information systems** → Data mining.

KEYWORDS

Knowledge Graph, Logical Reasoning, Complex Query Answering, Graph Neural Network

ACM Reference Format:

Chongzhi Zhang, Zhiping Peng, Junhao Zheng, and Qianli Ma. 2018. Conditional Logical Message Passing Transformer for Complex Query Answering. In *Proceedings of Make sure to enter the correct conference title from your rights confirmation email (Conference acronym 'XX)*. ACM, New York, NY, USA, 13 pages. <https://doi.org/XXXXXXXX.XXXXXXX>

1 INTRODUCTION

Knowledge graphs (KGs) store factual knowledge in the form of triples that can be utilized to support a variety of downstream tasks [42, 54, 58]. However, given that modern KGs are usually auto-generated [46] or built through crowd-sourcing [50], so real-world KGs [7, 9, 43] are often considered noisy and incomplete, which is also known as the Open World Assumption [22, 26]. Answering queries on such incomplete KGs is a fundamental yet challenging task. To alleviate the incompleteness of KGs, knowledge graph representation methods [8, 15, 44, 47], which can be viewed as neural link predictors [3], have been developed. They learn representations based on the available triples and generalize them to unseen triples. Such neural link predictors can answer one-hop atomic queries on incomplete KGs. But for multi-hop complex queries, the query-answering models need to perform multi-hop logical reasoning over incomplete KGs. That is, not only to utilize available knowledge to predict the unseen one but also execute logical operators, such as conjunction (\wedge), disjunction (\vee), and negation (\neg) [39, 57].

Recently, neural models [2, 39, 67] have been proposed to solve Complex Query Answering (CQA) over incomplete KGs. The complex queries that these models aim to address belong to an important subset of the first-order queries, specifically Existentially quantified First Order queries with a single free variable (EFO-1) [56, 57]. Such EFO-1 queries contain logical operators, including conjunction,

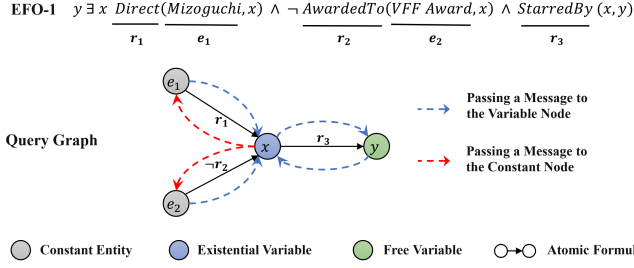


Figure 1: EFO-1 query and its query graph for the question “Who starred the films that were directed by Mizoguchi but never won a Venice Film Festival Award?”.

disjunction, and negation, as well as the existential quantifier (\exists) [39]. As shown in Figure 1, one can get the corresponding EFO-1 formula and query graph given a question. The query graph is a graphical representation of the EFO-1 query, where each edge is an atomic formula that contains a predicate with a (possible) negation operator, and each node represents an input constant entity or a variable. Most neural CQA models convert the query graph into the computation graph, where logical operators are replaced with corresponding set operators. These models embed the entity set into specific vector space [10, 39, 63, 67] and execute set operations parameterized by the neural networks according to the computation graph. However, these models cannot perform well on both one-hop and multi-hop queries simultaneously. They tend to be less effective than classical neural link predictors [47] on one-hop atomic queries [3, 56].

To this end, Logical Message Passing Neural Network (LMPNN) [56] proposes a message passing framework based on pre-trained neural link predictors. Specifically, for each edge in the query graph, LMPNN uses the pre-trained neural link predictor to infer an intermediate embedding for a node given neighborhood information. The intermediate embedding can be interpreted as a logical message passed by the neighbor on the edge. Figure 1 demonstrates the logical message passing with red/blue arrows. Then, LMPNN aggregates messages and updates node embeddings in a manner similar to Graph Isomorphism Network (GIN) [60]. While effective on both one-hop and multi-hop queries, LMPNN ignores the difference between constant and variable nodes. Logical message passing can be viewed as learning an embedding for the variable by utilizing information of constant entities. It makes this embedding similar or close to the embedding of the solution entity in the embedding space of the pre-trained neural link predictor. However, as shown by the red arrows in Figure 1, LMPNN also passes messages to constant entities with pre-trained embeddings and updates their embeddings, which we believe is unnecessary and experimentally demonstrated. In addition, for node embedding updating, despite the expressive power of GIN in graph structure learning [60], it cannot dynamically measure the importance of different logical messages. Furthermore, it is unclear whether the GIN-like approach can capture the implicit complex logical dependencies between messages received by a node and between messages and that node. Explicitly modeling the above implicit logical dependencies

while being able to measure the importance of different messages dynamically is an open challenge we take on in this paper.

We propose Conditional Logical Message Passing Transformer (CLMPT), a special Graph Neural Network (GNN) for CQA. Each CLMPT layer has two stages: (1) passing the logical message of each node to all of its neighbors that are not constant entity nodes; (2) updating the embedding of each variable node based on the logical messages received by the variable node. This means that during forward message passing, CLMPT does not use the pre-trained neural link predictor to infer the intermediate embeddings (i.e. logical messages) for constant entity nodes with pre-trained embeddings and does not update constant node embeddings. We call such a mechanism Conditional Logical Message Passing, where the condition depends on whether the node type is constant or variable. We empirically verified that it can reduce computational costs without affecting performance. Furthermore, CLMPT uses the transformer [49] to aggregate messages and update the corresponding node embedding. The self-attention mechanism in the transformer can dynamically measure the importance of different elements in the input and capture the interactions between any two elements. It allows us to explicitly model the logical dependencies between messages received by a node and between messages and that node. We conducted experiments on three popular KGs: FB15k [8], FB15k-237 [46], and NELL995 [59]. The experimental results show that CLMPT is a new state-of-the-art neural CQA model.

2 RELATED WORK

Neural Link Predictors. Reasoning over KGs with missing knowledge is one of the fundamental problems in Artificial Intelligence and has been widely studied. Traditional KG reasoning tasks such as link prediction [17, 47] are essentially one-hop atomic query problems. Representative methods for link prediction are knowledge graph representation methods [8, 15, 35, 44, 47, 62], which can be regarded as neural link predictors [3]. Specifically, they embed entities and relations into continuous vector spaces and predict unseen triples by scoring triples with a well-defined scoring function. Such latent feature models can effectively answer one-hop atomic queries over incomplete KGs. Other methods for link prediction include rule learning [40, 65], text representation learning [41, 51, 53], and GNNs [48, 66, 68].

Neural Complex Query Answering. Complex queries over KGs can be regarded as one-hop atomic queries combined with existential first-order logic operators. The scope of complex queries that existing works can answer is expanded from conjunctive queries [20, 24], to Existential Positive First-Order (EPFO) queries [3, 38], and more recently to the existential first-order [39], or more specifically to EFO-1 queries [56, 57]. Recently, neural query embedding (QE) models have been proposed to answer complex queries. Most QE models embed entity sets into specific continuous vector spaces with various forms, including geometric shapes [2, 12, 20, 27, 34, 38, 67], probabilistic distributions [11, 39, 63], fuzzy logic [10], and bounded histograms on uniform grids [55]. They represent the complex query in the form of the computation graph and perform neural set operations in the corresponding embedding spaces according to the computation graph. Such neural set operations are usually modeled by complex neural networks [45, 49]. In spite of getting

query embedding with neural set operations, other QE models represent the queries as graphs to embed queries with GNNs [1, 14] or Transformers [24, 28, 52]. However, these graph representation learning models only focus on EPFO queries, and how they handle the logical negation operator is unclear. Moreover, the aforementioned neural models are still less effective than a simple neural link predictor [47] on one-hop atomic queries.

There is also a class of neural CQA models based on pre-trained neural link predictors. CQD-CO [3] proposes a continuous optimization strategy that uses pre-trained neural link predictors [47] and logical t-norms [23] to solve complex queries. However, according to [56], CQD-CO performs badly on negative queries. LMPNN [56], which is most related to our work, proposes a logical message passing framework based on pre-trained neural link predictors. Through one-hop inference on atomic formulas, LMPNN performs bidirectional logical message passing on each edge in the query graph. However, such a mechanism ignores the difference between the constant node with a pre-trained embedding and the variable node whose embedding needs update. Our experimental results show that passing messages to the constant node and updating its embedding is unnecessary. In addition, at the node level, LMPNN aggregates the received logical messages and updates the node embeddings in a manner similar to GIN [60]. Despite the expressive power of GIN in graph structure learning, it cannot dynamically measure the importance of different messages. Whether such a GIN-like approach can capture the implicit logical dependencies between messages received by a node and between messages and that node remains unclear. By contrast, our work only performs conditional message passing on the query graph, which avoids unnecessary computation costs. Furthermore, by using the transformer [49] to aggregate the message and update the corresponding node embedding, our work can assign adaptive weights to elements in an input set consisting of received messages and the corresponding node and explicitly model logical dependencies between various elements.

Symbolic Integration Models. In addition to neural CQA models, some recent studies integrate symbolic information into neural models, which can be called symbolic integration models, also known as neural-symbolic models [3, 4, 6, 61, 69]. These models estimate the probability of whether each entity is the answer at each intermediate step in the process of multi-hop logical reasoning. This makes the size of the intermediate states for symbolic reasoning in symbolic integration models scale linearly with the size of the KG. Therefore, compared with neural CQA models where the intermediate embeddings are of fixed dimension, symbolic integration models require more computing resources and are more likely to suffer from scalability problems on large-scale KGs [37, 56].

3 BACKGROUND

Model-theoretic Concepts for Knowledge Graphs. A Knowledge Graph \mathcal{KG} consists of a set of entities \mathcal{V} and a set of relations \mathcal{R} . It can be defined as a set of triples $\mathcal{E} = (e_{h_i}, r_i, e_{t_i}) \subseteq \mathcal{V} \times \mathcal{R} \times \mathcal{V}$, namely $\mathcal{KG} = (\mathcal{V}, \mathcal{E}, \mathcal{R})$. A first-order language \mathcal{L} can be defined as $(\mathcal{F}, \mathcal{R}, \mathcal{C})$, where \mathcal{F} , \mathcal{R} , and \mathcal{C} are sets of symbols for functions, relations, and constants, respectively [56]. Under language $\mathcal{L}_{\mathcal{KG}}$, the \mathcal{KG} can be represented as a first-order logic knowledge base [3]. In this case, the relation symbols in \mathcal{R} denote

binary relations, the constant symbols in \mathcal{C} represent the entities, and the function symbol set satisfies $\mathcal{F} = \emptyset$. In other words, \mathcal{KG} is an $\mathcal{L}_{\mathcal{KG}}$ -structure, where each entity $e \in \mathcal{V}$ is also a constant $c \in \mathcal{C} = \mathcal{V}$ and each relation $r \in \mathcal{R}$ is a set $r \subseteq \mathcal{V} \times \mathcal{V}$. We have $r(t_1, t_2) = True$ when $(t_1, t_2) \in r$. An atomic formula is either $r(t_1, t_2)$ or $\neg r(t_1, t_2)$, where t_i is a term that can be a constant or a variable, and r is a relation that can be viewed as a binary predicate [3]. A variable is a bound variable when associated with a quantifier. Otherwise, it is a free variable. By adding connectives (conjunction \wedge , disjunction \vee , and negation \neg) to such atomic formulas and adding quantifiers (existential \exists and universal \forall) to variables, we can inductively define the first order formula [33, 56].

EFO-1 Queries. In this paper, we consider Existential First Order queries with a single free variable (EFO-1) [56, 57]. Such EFO-1 queries are an important subset of first-order queries, using existential quantifier, conjunction, disjunction, and atomic negation. Following the previous studies [38, 39, 56], we define the EFO-1 query as the first order formula in the following Disjunctive Normal Form (DNF) [13]:

$$q[y, x_1, \dots, x_k] = \exists x_1, \dots, \exists x_k (a_1^1 \wedge \dots \wedge a_{n_1}^1) \vee \dots \vee (a_1^d \wedge \dots \wedge a_{n_d}^d), \quad (1)$$

where y is the only free variable, x_1, \dots, x_k are existential variables. a_j^i are atomic formulas that can be either negated or not:

$$a_j^i = \begin{cases} r(e_c, v) \text{ or } r(v, v') \\ \neg r(e_c, v) \text{ or } \neg r(v, v') \end{cases}, \quad (2)$$

where $e_c \in \mathcal{V}$ is an input constant entity, $v, v' \in \{y, x_1, \dots, x_k\}$ are variables, $v \neq v'$. To address the EFO-1 query q , the corresponding answer entity set $\llbracket q \rrbracket \subseteq \mathcal{V}$ needs to be determined, where $\llbracket q \rrbracket$ is a set of entities such that $e \in \llbracket q \rrbracket$ iff $q[y = e, x_1, \dots, x_k] = True$. In particular, since we use DNF to represent the first order formula, the Equation 1 can also be expressed as the disjunction of conjunctive queries:

$$q[y, x_1, \dots, x_k] = CQ_1(y, x_1, \dots, x_k) \vee \dots \vee CQ_d(y, x_1, \dots, x_k), \quad (3)$$

where $CQ_i = \exists x_1, \dots, \exists x_k a_1^i \wedge \dots \wedge a_{n_i}^i$ is a conjunctive query. According to [38, 56], we can get the answer set $\llbracket q \rrbracket$ by taking the union of the answer sets of each conjunctive query, namely $\llbracket q \rrbracket = \bigcup_{i=1}^d \llbracket CQ_i \rrbracket$. This means that solving all conjunctive queries $CQ_i, 1 \leq i \leq d$ yields the answer set $\llbracket q \rrbracket$ for the EFO-1 query q . Such DNF-based processing can solve complex queries involving disjunction operators in a scalable way [36–38].

Query Graph. Since disjunctive queries can be solved in a scalable manner by transforming queries into the disjunctive normal form, it is only necessary to define query graphs for conjunctive queries. We follow previous works [38, 56] and represent the conjunctive query as the query graph where the terms are represented as nodes connected by the atomic formulas. That is, each edge in the query graph is an atomic formula. According to the definition in Equation 2, an atomic formula contains relations, negation information, and terms. Therefore, each node in the query graph is either a constant entity or a free or existential variable, as illustrated in Figure 1.

Neural Link Predictors. A neural link predictor has a corresponding scoring function that is used to learn the embeddings of entities and relations in KG. For a triple, the embeddings of the head entity, relation, and tail entity are h , r , and t , respectively. The scoring function $\phi(h, r, t)$ can calculate the likelihood score of whether the triple exists. By using the scoring function $\phi(h, r, t)$ and the sigmoid function σ , neural link predictors can produce a continuous truth value $\psi(h, r, t) \in [0, 1]$ for a triple. For example, the scoring function of ComplEx [47] is as follows:

$$\phi(h, r, t) = \text{Re}(\langle h \otimes r, \bar{t} \rangle), \quad (4)$$

where \otimes represents the element-wise complex number multiplication, $\langle \cdot, \cdot \rangle$ is the complex inner product, and Re means taking the real part of a complex number. Based on $\phi(h, r, t)$, we can obtain the corresponding truth value:

$$\psi(h, r, t) = \sigma(\phi(h, r, t)). \quad (5)$$

In this work, the neural link predictor handles not only specific entity embeddings but also variable embeddings. That is, the embeddings h, t correspond to embedding of terms, which can be the embeddings of constant entities or the embeddings of variables. Following previous works [3, 56], in our work, we use ComplEx-N3 [25, 47] as the neural link predictor of CLMPT.

One-hop Inference on Atomic Formulas. As shown in Figure 1, each edge in a query graph is an atomic formula containing the information of relation, logical negation, and terms. Passing a logical message on an edge is essentially an operation of utilizing this information to perform one-hop inference on an atomic formula. On each edge, when a node is at the head position, its neighbor is at the tail position, and vice versa. A logical message passed from a neighbor to a node is essentially an intermediate embedding of that node. Prior work [56] proposes to obtain the intermediate embeddings of nodes by one-hop inference that maximizes the continuous truth value of the (negated) atomic formulas. Specifically, a logical message encoding function ρ is proposed to perform one-hop inference. Such function has four input parameters, including neighbor embedding, relation embedding, direction information ($h \rightarrow t$ or $t \rightarrow h$), and logical negation information (0 for no negation and 1 for with negation), and it has four cases depending on the input parameters. Given the tail embedding t and relation embedding r on a non-negated atomic formula, ρ is formulated in the form of continuous truth value maximization to infer the head embedding \hat{h} :

$$\hat{h} = \rho(t, r, t \rightarrow h, 0) := \arg \max_{x \in \mathcal{D}} \psi(x, r, t), \quad (6)$$

where \mathcal{D} is the search domain for the embedding x . Similarly, the tail embedding \hat{t} on a non-negated atomic formula can be inferred given h and r :

$$\hat{t} = \rho(h, r, h \rightarrow t, 0) := \arg \max_{x \in \mathcal{D}} \psi(h, r, x). \quad (7)$$

According to the fuzzy logic negator [19], one has $\psi(h, \neg r, t) = 1 - \psi(h, r, t)$. Therefore, the estimation of head and tail embeddings on negated atomic formulas can be defined as follows:

$$\hat{h} = \rho(t, r, t \rightarrow h, 1) := \arg \max_{x \in \mathcal{D}} [1 - \psi(x, r, t)], \quad (8)$$

$$\hat{t} = \rho(h, r, h \rightarrow t, 1) := \arg \max_{x \in \mathcal{D}} [1 - \psi(h, r, x)]. \quad (9)$$

For the situation where ComplEx-N3 [25, 47] is selected as the neural link predictor, according to the propositions and proofs in [56], the logical message encoding function ρ has the following closed-form with respect to the complex embedding r and t when inferring the head embedding \hat{h} on a non-negated atomic formula:

$$\begin{aligned} \rho(t, r, t \rightarrow h, 0) &= \arg \max_{x \in \mathbb{C}^d} \{ \text{Re}(\langle \bar{r} \otimes t, \bar{x} \rangle) - \lambda \|x\|^3 \} \\ &= \frac{\bar{r} \otimes t}{\sqrt{3\lambda} \|\bar{r} \otimes t\|}, \end{aligned} \quad (10)$$

Similarly, for the other three cases, the encoding functions ρ are as follows:

$$\rho(h, r, h \rightarrow t, 0) = \frac{r \otimes h}{\sqrt{3\lambda} \|r \otimes h\|}, \quad (11)$$

$$\rho(t, r, t \rightarrow h, 1) = \frac{-\bar{r} \otimes t}{\sqrt{3\lambda} \|\bar{r} \otimes t\|}, \quad (12)$$

$$\rho(h, r, h \rightarrow t, 1) = \frac{-r \otimes h}{\sqrt{3\lambda} \|r \otimes h\|}. \quad (13)$$

For Equations 10–13, the λ is a hyperparameter. In our work, we follow prior work [56] and use the above logical message encoding function ρ to compute messages passed to the variable nodes.

4 PROPOSED METHOD

In this section, we propose Conditional Logical Message Passing Transformer (CLMPT) to answer complex queries. As a special message passing neural network [18], each CLMPT layer has two stages: (1) passing the logical message of each node to all of its neighbors that are not constant entity nodes; (2) updating the embedding of each variable node based on the messages received by the variable node. Figure 2 illustrates how these two stages work using the query graph in Figure 1. Then, we can use the final layer embedding of the free variable node to predict the answer entities to the corresponding query. In the following subsections, we first describe how each layer of CLMPT performs conditional logical message passing and updates the variable node embeddings. After that, we represent the training objective of our method. Finally, we introduce how to answer complex queries with CLMPT.

4.1 Conditional Logical Message Passing

A query graph contains two types of nodes: constant entity nodes and variable nodes. We decide whether to pass logical messages to a node based on its type. Specifically, for any neighbor of a node, when the neighbor is a variable node, we use the logical message encoding function ρ to calculate the corresponding message and pass it to the neighbor; when the neighbor is a constant entity node, we do not pass the logical message to it. Figure 2 (a) demonstrates the conditional logical message passing with blue arrows. Every node in the query graph except the constant entity nodes receives the logical message from all of its neighbors.

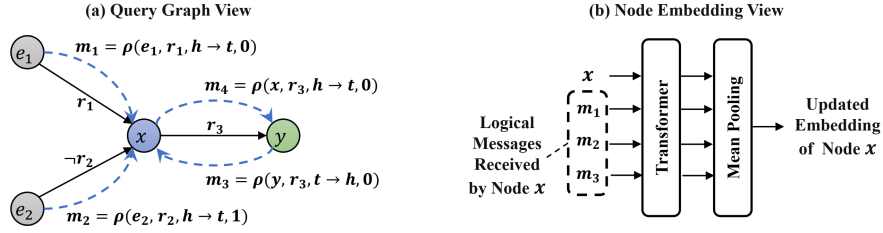


Figure 2: An illustration of the two-stage procedures of CLMPT. (a) Passing the logical message to the variable node in the neighborhood. (b) Updating the existential variable node embedding with the received messages and a transformer encoder. Similarly, such a node embedding update scheme is applied to other variable nodes, such as the free variable node y .

4.2 Node Embedding Conditional Update Scheme

For a constant entity node, we denote its embedding at the l -th layer as $z_e^{(l)}$ and let $z_v^{(l)}$ be the embedding of a variable node at the l -th layer. Next, we discuss how to calculate the $z_e^{(l)}$ and $z_v^{(l)}$ from the input layer $l = 0$ to latent layers $l > 0$. For a constant entity node, $z_e^{(0)}$ is the corresponding entity embedding in the pre-trained neural link predictor, which can be frozen or optimized continuously. For $z_v^{(0)}$, we follow previous works [56] and assign two learnable embeddings v_x, v_y for the existential variable node x and the free variable node y respectively, and set that all existential variable nodes x_i share one v_x , namely $z_{x_i}^{(0)} = v_x$ and $z_y^{(0)} = v_y$. Similar to conditional logical message passing, for updating the node embeddings, we also do not consider constant entity nodes. That is, we only update node embeddings for variable nodes in the query graph. Thus, the embeddings of the constant entity nodes are the same at each layer, namely $z_e^{(l)} = z_e^{(0)}$. While for $z_v^{(l)}$, we use the corresponding information from the $(l-1)$ -th layer to update it. Specifically, for a variable node v , we represent its neighbor set in the query graph as $\mathcal{N}(v)$. For each neighbor node $n \in \mathcal{N}(v)$, one can obtain information about the edge (i.e., the atomic formula) between n and v , which contains the neighbor embedding $z_n^{(l-1)} \in \mathcal{D}$, the relation $r_{nv} \in \mathcal{R}$, the direction $D_{nv} \in \{h \rightarrow t, t \rightarrow h\}$, and the negation indicator $Neg_{nv} \in \{0, 1\}$. Based on the edge information, we can use the logical message encoding function ρ to compute the logical message $m^{(l)}$ that n passes to v :

$$m^{(l)} = \rho(z_n^{(l-1)}, r_{nv}, D_{nv}, Neg_{nv}). \quad (14)$$

Let k_v be the number of neighbor nodes in $\mathcal{N}(v)$, where $k_v \geq 1$. For the variable node v , it receives k_v logical messages from k_v neighbors: $m_1^{(l)}, \dots, m_{k_v}^{(l)}$. We use the transformer [49] to encode the input set consisting of these logical messages and the variable node embedding $z_v^{(l-1)}$ to obtain the updated embedding of node v :

$$z_v^{(l)} = \text{Mean}(\text{TE}^{(l)}(m_1^{(l)}, \dots, m_{k_v}^{(l)}, z_v^{(l-1)})), \quad (15)$$

where Mean is a mean pooling layer, TE is a standard transformer encoder. Through the self-attention mechanism in the transformer, we can explicitly model the complex logical dependencies between various elements in the input set and dynamically measure the importance of different elements. Figure 2 (b) shows how to obtain

the updated embedding of the existential variable node x through the encoding process defined by Equation 15.

4.3 Training Objective

We use the Noisy Contrastive Estimation (NCE) loss proposed in [32] to train CLMPT. Specifically, we denote the positive data as $\{(a_i, q_i)\}_{i=1}^N$, where $a_i \in \llbracket q_i \rrbracket$. Our optimization involves K uniformly sampled noisy answers from the entity set. The training objective is as follows:

$$L_{NCE} = -\frac{1}{N} \sum_{i=1}^N \log \left[\frac{F(z_{a_i}, z(q_i), T)}{F(z_{a_i}, z(q_i), T) + \sum_{k=1}^K F(z_{n_{ik}}, z(q_i), T)} \right], \quad (16)$$

$$F(x, y, z) = \exp[\cos(x, y)/z], \quad (17)$$

where $\cos(\cdot, \cdot)$ is the cosine similarity, T is a hyperparameter, z_{a_i} is the embedding of positive answer a_i , $z_{n_{ik}}$ is the embedding of the k -th noisy samples, and $z(q_i)$ is the embedding of the predicted answer to the query q_i , corresponding to the embedding of the free variable of the query q_i at the final layer of CLMPT.

4.4 Answering Complex Queries with CLMPT

For a complex query defined in Equation 3, i.e., a DNF query, we follow the previous works [38, 39] and use DNF-based processing to get answer entities. Specifically, we estimate the predicted answer embeddings for each sub-conjunctive query of the complex query. Then, the answer entities are ranked by the maximal cosine similarity against these predicted answer embeddings. Therefore, CLMPT only needs to consider the query graph of the conjunctive query.

For a given conjunctive query q , let the depth of CLMPT be L , and we apply the CLMPT layers L times to the query graph of q . Then, we can obtain the free variable embedding $z_y^{(L)}$ at the final layer. We use $z_y^{(L)}$ as the embedding of the predicted answer entity, namely $z(q) = z_y^{(L)}$. Based on the cosine similarity between $z(q)$ and the entity embeddings in the pre-trained neural link predictor, we can rank the entities to retrieve answers. For the depth L , according to the analyses in [56], L should be the largest distance between the constant entity nodes and the free variable node to ensure the free variable node successfully receives all logical messages from the constant entity nodes. This means L is not determined, and L should change dynamically with different conjunctive query types.

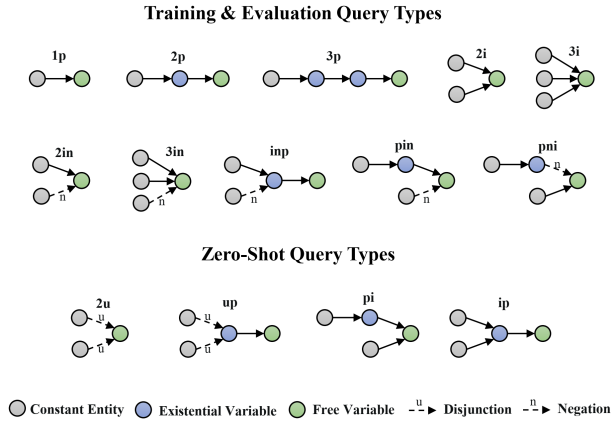


Figure 3: All the query types considered in our experiments, where p , i , u , and n represent projection, intersection, union, and negation, respectively. The naming of each query type reflects how they were generated in the BetaE paper [39].

Thus, we follow prior work [56] and assume all L CLMPT layers share the same transformer encoder.

In this case, the parameters in CLMPT include two embeddings for existential and free variables, a transformer encoder, and the parameters in the pre-trained neural link predictor. For the pre-trained neural link predictor, it can be frozen or not. In our work, we continue to optimize pre-trained neural link predictors by default, that is, we do not freeze pre-trained embeddings of entities and relations.

5 EXPERIMENTS

5.1 Experimental Settings

5.1.1 Datasets and Queries. We evaluate our method on three commonly-used standard knowledge graphs: FB15k [8], FB15k-237 [46], and NELL995 [59]. For a fair comparison with previous works, we use the datasets of complex queries proposed by BetaE [39], which consist of five conjunctive query types ($1p/2p/3p/2i/3i$), five query types with atomic negations ($2in/3in/inp/pin/pni$), and four zero-shot query types ($pi/ip/2u/up$), as illustrated in Figure 3. The datasets provided by BetaE introduce complex queries with hard answers that cannot be obtained by traversing the KG directly. That is, the evaluation focuses on discovering such hard answers to complex queries. We follow previous works [39, 56, 67] and train our model with five conjunctive query types and five query types with atomic negations. When evaluating the model, we consider all query types including the four zero-shot query types. The statistics for each dataset are presented in Table 1. More details about the datasets can be found in Appendix A.

5.1.2 Evaluation Protocol. The evaluation scheme follows the previous works [39, 56], which divides the answers to each complex query into easy and hard sets. For test and validation splits, we define hard answers as those that cannot be obtained by direct graph traversal on KG. In order to get these hard answers, the model is required to impute at least one missing edge, which means the model

Table 1: Statistics of different query types used in the benchmark datasets.

Split	Query Types	FB15k	FB15k-237	NELL995
Train	1p, 2p, 3p, 2i, 3i	273,710	149,689	107,982
	2in, 3in, inp, pin, pni	27,371	14,968	10,798
Valid	1p	59,078	20,094	16,910
	Others	8,000	5,000	4,000
Test	1p	66,990	22,804	17,021
	Others	8,000	5,000	4,000

needs to complete non-trivial reasoning [38, 39]. Specifically, for each hard answer of a query, we rank it against non-answer entities based on their cosine similarity with the free variable embedding of the query and calculate the Mean Reciprocal Rank (MRR).

5.1.3 Baselines. We consider the state-of-the-art neural complex query answering models for EFO-1 queries in recent years as our baselines to compare: BetaE [39], ConE [67], Q2P [5], MLP [2], GammaE [63], CylE [34], CQD-CO [3], and LMPNN [56], where CQD-CO and LMPNN use pre-trained neural link predictor, while other models do not. In addition, some other neural CQA models cannot handle logical negation operators, such as BIQE [24], PREM [11], kgTransformer [28], etc., which use the EPFO queries generated by Q2B [38] for training and evaluation. We compare these works on the Q2B datasets in Appendix C. We also compare our work with symbolic integration CQA models in Appendix E.

5.1.4 Model Details. Following LMPNN [56] and CQD-CO [3], we choose ComplEx-N3 [25, 47] as the neural link predictor in our work and use the ComplEx-N3 checkpoints released by CQD-CO to conduct experiments. The rank of ComplEx-N3 is 1,000, and the epoch for the checkpoints is 100. For all datasets, we use a two-layer transformer encoder with eight self-attention heads, where the dimension of the hidden layer of the feed-forward network (FFN) in the transformer is 8,192. For the training objective, the negative sample size K is 128, and T is chosen as 0.05 for FB15k-237 and FB15k and 0.1 for NELL995. For more details about the implementation and experiments, please refer to Appendix B.

5.2 Main Results

Table 2 shows the MRR results of CLMPT and neural CQA baselines about answering EFO-1 queries over three KGs. It is found that CLMPT reaches the best performance on average for EPFO queries across all three datasets. Compared with LMPNN, which is most relevant to our work, CLMPT achieves average performance improvements of 8.9%, 7.5%, and 2.0% for EPFO queries on FB15k, FB15K-237, and NELL995, respectively. Since conditional logical message passing has little impact on the model performance (it will be later discussed in Section 5.3.1), these performance improvements are mainly due to the transformer-based node embedding update scheme. This shows that this approach, which explicitly models dependencies between input elements by assigning adaptive weights to the messages and the corresponding node through the self-attention mechanism, is more suitable for the logical query graphs of EPFO queries than the GIN-like approach. For the negative queries, CLMPT achieves the best average performance on

Table 2: The MRR results of baselines and our model over three KGs. Avg_p represents the average score of EPFO queries and Avg_n denote the average score of queries with negation. The boldface indicates the best results, and the second-best ones are marked with underlines.

Dataset	Model	1p	2p	3p	2i	3i	pi	ip	2u	up	2in	3in	inp	pin	pni	Avg _p	Avg _n	
FB15k	BetaE	65.1	25.7	24.7	55.8	66.5	43.9	28.1	40.1	25.2	14.3	14.7	11.5	6.5	12.4	41.6	11.8	
	ConE	73.3	33.8	29.2	64.4	73.7	50.9	35.7	<u>55.7</u>	31.4	17.9	18.7	12.5	9.8	15.1	49.8	14.8	
	Q2P	82.6	30.8	25.5	65.1	74.7	49.5	34.9	32.1	26.2	<u>21.9</u>	20.8	12.5	8.9	<u>17.1</u>	46.8	16.4	
	MLP	67.1	31.2	27.2	57.1	66.9	45.7	33.9	38.0	28.0	17.2	17.8	13.5	9.1	15.2	43.9	14.5	
	GammaE	76.5	36.9	<u>31.4</u>	65.4	75.1	<u>53.9</u>	39.7	53.5	30.9	20.1	20.5	13.5	<u>11.8</u>	<u>17.1</u>	51.3	16.6	
	CyIE	78.8	37.0	30.9	66.9	75.7	53.8	40.8	59.4	<u>33.5</u>	15.7	16.3	13.7	7.8	13.9	<u>53.0</u>	13.5	
	(Using pre-trained neural link predictor)																	
	CQD-CO	89.4	27.6	15.1	63.0	65.5	46.0	35.2	42.9	23.2	0.2	0.2	4.0	0.1	18.4	45.3	4.6	
	LMPNN	85.0	<u>39.9</u>	28.6	<u>68.2</u>	<u>76.5</u>	46.7	<u>43.0</u>	36.7	31.4	29.1	29.4	<u>14.9</u>	10.2	16.4	50.6	20.0	
	CLMPT	<u>86.1</u>	43.3	33.9	69.1	78.2	55.1	46.6	46.1	37.3	21.2	<u>22.9</u>	17.0	13.0	15.3	55.1	<u>17.9</u>	
FB15k-237	BetaE	39.0	10.9	10.0	28.8	42.5	22.4	12.6	12.4	9.7	5.1	7.9	7.4	3.6	3.4	20.9	5.4	
	ConE	41.8	12.8	<u>11.0</u>	32.6	47.3	25.5	14.0	<u>14.5</u>	10.8	5.4	8.6	7.8	4.0	3.6	23.4	5.9	
	Q2P	39.1	11.4	10.1	32.3	47.7	24.0	14.3	<u>8.7</u>	9.1	4.4	9.7	7.5	4.6	3.8	21.9	6.0	
	MLP	42.7	12.4	10.6	31.7	43.9	24.2	14.9	13.7	9.7	6.6	10.7	8.1	4.7	4.4	22.6	6.9	
	GammaE	43.2	13.2	<u>11.0</u>	33.5	47.9	<u>27.2</u>	15.9	13.9	10.3	6.7	9.4	8.6	<u>4.8</u>	4.4	24.0	6.8	
	CyIE	42.9	<u>13.3</u>	11.3	<u>35.0</u>	<u>49.0</u>	27.0	15.7	15.3	11.2	4.9	8.3	<u>8.2</u>	3.7	3.4	<u>24.5</u>	5.7	
	(Using pre-trained neural link predictor)																	
	CQD-CO	46.7	10.3	6.5	23.1	29.8	22.1	16.3	14.2	8.9	0.2	0.2	2.1	0.1	6.1	19.8	1.7	
	LMPNN	<u>45.9</u>	13.1	10.3	34.8	48.9	22.7	<u>17.6</u>	13.5	10.3	8.7	<u>12.9</u>	7.7	4.6	<u>5.2</u>	24.1	<u>7.8</u>	
	CLMPT	45.7	13.7	11.3	37.4	52.0	28.2	19.0	14.3	<u>11.1</u>	<u>7.7</u>	13.7	8.0	5.0	5.1	25.9	7.9	
NELL995	BetaE	53.0	13.0	11.4	37.6	47.5	24.1	14.3	12.2	8.5	5.1	7.8	10.0	3.1	3.5	24.6	5.9	
	ConE	53.1	16.1	13.9	40.0	50.8	26.3	17.5	15.3	11.3	5.7	8.1	10.8	3.5	3.9	27.2	6.4	
	Q2P	56.5	15.2	12.5	35.8	48.7	22.6	16.1	11.1	10.4	5.1	7.4	10.2	3.3	3.4	25.5	6.0	
	MLP	55.2	16.8	14.9	36.4	48.0	22.7	18.2	14.7	11.3	5.1	8.0	10.0	3.6	3.6	26.5	6.1	
	GammaE	55.1	17.3	14.2	41.9	51.1	26.9	18.3	15.1	11.2	6.3	<u>8.7</u>	11.4	4.0	4.5	27.9	<u>7.0</u>	
	CyIE	56.5	17.5	15.6	41.4	<u>51.2</u>	27.2	19.6	15.7	12.3	5.6	7.5	11.2	3.4	3.7	28.5	6.3	
	(Using pre-trained neural link predictor)																	
	CQD-CO	60.8	<u>18.3</u>	13.2	36.5	43.0	30.0	22.5	<u>17.6</u>	13.7	0.1	0.1	4.0	0.0	5.2	28.4	1.9	
	LMPNN	<u>60.6</u>	22.1	<u>17.5</u>	40.1	50.3	<u>28.4</u>	24.9	17.2	<u>15.7</u>	8.5	10.8	12.2	<u>3.9</u>	<u>4.8</u>	<u>30.7</u>	8.0	
	CLMPT	58.9	22.1	18.4	<u>41.8</u>	51.9	28.8	<u>24.4</u>	18.6	16.2	<u>6.6</u>	8.1	<u>11.8</u>	3.8	4.5	31.3	<u>7.0</u>	

FB15k-237 and sub-optimal performance on the remaining two KGs. One potential explanation for these sub-optimal results is that the transformer architecture lacks inductive biases and relies more on the training data. As shown in the statistics in Table 1, the number of negative queries in the training set is an order of magnitude less than the EPFO queries, which may lead to the tendency of the transformer encoder to learn the patterns relevant to answering EPFO queries, resulting in insufficient modeling of relevant patterns that answer negative queries.

5.3 ABLATION STUDY

5.3.1 Conditional Logical Message Passing. The logical message passing mechanism can be viewed as learning an embedding for the variable by utilizing information of constant entities. It makes this embedding similar to the embedding of the solution entity in the embedding space of the pre-trained neural link predictor. As in the previous analyses, we argue that for a constant node with the corresponding entity embedding, it is unnecessary to update its embedding in the forward passing of the model. To verify this, we conduct experiments on whether to pass messages to the constant node and update its embedding, and the results are

Table 3: The average MRR results of models with or without conditional logical message passing on answering EFO-1 queries. ↓Memory and ↓Time represent the GPU memory usage reduction and time savings with conditional logical message passing, respectively. The boldface indicates the best results.

Dataset	Model	Avg _p	Avg _n	↓Memory	↓Time
FB15k-237	LMPNN	24.1	7.8		
	LMPNN w/ C	24.3	7.8	↓1.2%	↓5.0%
	CLMPT w/o C	25.8	7.7		
	CLMPT	25.9	7.9	↓9.6%	↓12.3%
NELL995	LMPNN	30.7	8.0		
	LMPNN w/ C	31.0	8.2	↓0.6%	↓8.3%
	CLMPT w/o C	31.4	7.0		
	CLMPT	31.3	7.0	↓8.0%	↓11.0%

shown in Table 3, where "w/ C" indicates "with conditional logical message passing" and "w/o C" indicates "without conditional logical message passing". From the experimental results, the performance

Table 4: The MRR results of different hyperparameter settings and different pooling approaches. The best results are bold.

Model	1p	2p	3p	2i	3i	pi	ip	2u	up	2in	3in	inp	pin	pni	Avg _p	Avg _n
<i>TE</i> layer = 1	45.8	13.2	10.9	37.3	51.9	27.7	18.2	14.6	10.9	7.7	13.3	8.1	5.3	4.5	25.6	7.8
<i>TE</i> layer = 3	45.8	13.9	11.4	37.3	51.8	29.0	19.2	14.4	11.2	7.6	13.1	8.1	5.0	4.9	26.0	7.7
$d_{\text{FFN}} = 4096$	45.8	13.5	11.1	37.3	51.7	27.9	18.6	14.3	11.2	7.7	13.2	8.1	5.1	4.9	25.7	7.8
self-attention head = 4	45.9	13.6	11.3	37.4	52.0	28.1	18.7	14.6	11.3	7.4	13.1	8.1	5.0	4.8	25.9	7.7
self-attention head = 16	45.0	12.8	10.3	36.4	50.4	26.8	18.0	14.5	10.6	7.5	12.9	7.7	5.2	4.3	25.0	7.5
$T = 0.01$	45.8	12.9	10.3	35.1	48.9	26.4	16.8	14.1	10.3	7.1	10.8	7.4	5.6	4.0	24.5	7.0
$T = 0.1$	44.9	13.5	10.7	34.4	47.2	26.5	18.7	15.6	11.1	7.6	10.2	8.1	4.2	5.8	24.7	7.2
Max Pooling	46.1	13.8	11.1	36.8	50.5	26.0	17.5	14.4	11.1	5.1	9.5	7.3	3.7	3.4	25.2	5.8
Sum Pooling	45.9	13.8	11.0	37.5	51.9	28.5	18.7	14.3	11.3	7.6	13.6	8.2	5.0	4.9	25.9	7.9
Default Setting	45.7	13.7	11.3	37.4	52.0	28.2	19.0	14.3	11.1	7.7	13.7	8.0	5.0	5.1	25.9	7.9

of LMPNN with conditional logical message passing on the two KGs is not reduced but improved. CLMPT achieves better results on FB15k-237 than the variant that does not use conditional logical message passing, only slightly underperforming the variant on the EPFO queries of NELL995. In addition, we evaluate how much unnecessary computational cost the conditional logical message passing mechanism can avoid on an RTX 3090 GPU. Specifically, we calculate the relative percentage of the reduction in GPU memory usage and the relative percentage of training time saved:

$$\downarrow \text{Memory} = (usage_{woC} - usage_C) / usage_{woC}, \quad (18)$$

$$\downarrow \text{Time} = (t_{woC} - t_C) / t_{woC}, \quad (19)$$

where $usage_C$ and t_C respectively refer to the GPU memory usage and the required training time when the model uses conditional logical message passing, while $usage_{woC}$ and t_{woC} correspond to the situation without conditional logical message passing. As shown in Table 3, conditional logical message passing reduces computational costs without significantly negatively impacting model performance. In particular, the computational cost reduction is particularly significant for CLMPT, which uses the more complex transformer architecture. The above results confirm our view that the model does not need to consider the constant entity nodes in the query graph during the forward message passing.

5.3.2 Hyperparameters and Pooling Approaches. We evaluate the performance of CLMPT with different hyperparameter settings and pooling approaches on FB15k-237. The default setting we adopted is described in Section 5.1.4. As is shown in Table 4, regardless of reducing the number of transformer encoder layers or halving the dimensions of the hidden layer of the FFN, the model still achieves the best performance than the baselines on FB15k-237, which reflects the effectiveness of our proposed method. When the number of transformer encoder layers increases, the performance changes little, meaning the two-layer transformer encoder is sufficient. In addition, we can find that T in NCE loss is very important to the performance. When T is 0.01 or 0.1, the performance of the model is still competitive on EPFO queries, but there is a large gap with the average performance under the default settings. For the pooling approaches, we evaluate max pooling and sum pooling. The experimental results show max pooling does not perform as well as sum pooling and mean pooling.

5.3.3 Frozen or Trainable Neural Link Predictors. For the pre-trained neural link predictor, it can be frozen or trainable. As mentioned above (see Section 4.4), in our work, we optimize all parameters in the pre-trained neural link predictor by default. It is worth noting that the pre-trained neural link predictor is frozen in LMPNN. In order to explore the impact of freezing the pre-trained neural link predictor on model performance, we conduct experiments on three KGs, and the results are shown in Table 5.

Table 5: The average MRR results for experiments on whether to freeze the Neural Link Predictor (NLP). The boldface indicates the best results.

Dataset	Model	Frozen NLP		Trainable NLP	
		Avg _p	Avg _n	Avg _p	Avg _n
FB15k	LMPNN	50.6	20.0	51.5	18.9
	CLMPT	54.2	17.3	55.1	17.9
FB15k-237	LMPNN	24.1	7.8	24.4	7.5
	CLMPT	25.4	7.7	25.9	7.9
NELL995	LMPNN	30.7	8.0	30.1	7.9
	CLMPT	32.0	6.8	31.3	7.0

For LMPNN, using frozen neural link predictors performs better than using trainable ones, except for EPFO queries on FB15k and FB15k-237. Therefore, in the main results, we only compare the MRR results of LMPNN using frozen neural link predictors, i.e. the results reported in the original paper [56]. For CLMPT, with the exception of EPFO queries on NELL995, CLMPT using the trainable neural link predictor performs relatively better. Thus, we continue to optimize the pre-trained neural link predictor on complex queries by default. For these results of CLMPT, according to the progress of pre-training and fine-tuning paradigms [16, 29], one possible reason is that the neural link predictor is pre-trained on one-hop queries, and tuning its parameters on complex queries can make the embeddings of entities and relations more suitable for the patterns and characteristics of CQA. The better performance of LMPNN using trainable neural link predictors on EPFO queries of FB15k and FB15K-237 can also support our argument to some extent because the number of EPFO queries in the datasets is much more than negative ones; in this case, the model is more inclined to learn patterns that answer EPFO queries.

Although CLMPT, which uses the trainable neural link predictor, has more training parameters, it still significantly outperforms LMPNN on EPFO queries across all datasets when the neural link predictor is frozen. This reflects the effectiveness of CLMPT. For more experimental analyses of the model parameters, please refer to Appendix D.

6 CONCLUSION

In this paper, we propose CLMPT, a special message passing neural network, to answer complex queries over KGs. Based on one-hop inference by pre-trained neural link predictor on atomic formulas, CLMPT performs logical message passing conditionally on the node type. In the ablation study, we verify that this conditional message passing mechanism can effectively reduce the computational costs and even improve the performance of the model to some extent. Furthermore, CLMPT uses the transformer to aggregate messages and update the corresponding node embedding. Through the self-attention mechanism, CLMPT can explicitly model logical dependencies between messages received by a node and between messages and that node by assigning adaptive weights to the messages and the node. The experimental results show that CLMPT achieves a strong performance through this transformer-based node embedding update scheme. Future work may integrate symbolic information into CLMPT to improve the performance in answering negative queries.

REFERENCES

- [1] Dimitrios Alivanistos, Max Berrendorf, Michael Cochez, and Mikhail Galkin. 2022. Query Embedding on Hyper-Relational Knowledge Graphs. In *International Conference on Learning Representations*. <https://openreview.net/forum?id=4rLw09TgRw9>
- [2] Alfonso Amayuelas, Shuai Zhang, Susie Xi Rao, and Ce Zhang. 2022. Neural Methods for Logical Reasoning over Knowledge Graphs. In *Proceedings of the Tenth International Conference on Learning Representations 2022*.
- [3] Erik Arakelyan, Daniel Daza, Pasquale Minervini, and Michael Cochez. 2020. Complex Query Answering with Neural Link Predictors. In *International Conference on Learning Representations*.
- [4] Erik Arakelyan, Pasquale Minervini, Daniel Daza, Michael Cochez, and Isabelle Augenstein. 2023. Adapting Neural Link Predictors for Data-Efficient Complex Query Answering. In *Thirty-seventh Conference on Neural Information Processing Systems*.
- [5] Jiaxin Bai, Zihao Wang, Hongming Zhang, and Yangqiu Song. 2022. Query2Particles: Knowledge Graph Reasoning with Particle Embeddings. In *Findings of the Association for Computational Linguistics: NAACL 2022*. 2703–2714.
- [6] Yushi Bai, Xin Lv, Juanzi Li, and Lei Hou. 2023. Answering complex logical queries on knowledge graphs via query computation tree optimization. In *International Conference on Machine Learning*. PMLR, 1472–1491.
- [7] Kurt Bollacker, Colin Evans, Praveen Paritosh, Tim Sturge, and Jamie Taylor. 2008. Freebase: a collaboratively created graph database for structuring human knowledge. In *Proceedings of the 2008 ACM SIGMOD international conference on Management of data*. 1247–1250.
- [8] Antoine Bordes, Nicolas Usunier, Alberto Garcia-Duran, Jason Weston, and Oksana Yakhnenko. 2013. Translating embeddings for modeling multi-relational data. *Advances in neural information processing systems* 26 (2013).
- [9] Andrew Carlson, Justin Betteridge, Bryan Kisiel, Burr Settles, Estevam Hruschka, and Tom Mitchell. 2010. Toward an architecture for never-ending language learning. In *Proceedings of the AAAI conference on artificial intelligence*, Vol. 24. 1306–1313.
- [10] Xuelu Chen, Ziniu Hu, and Yizhou Sun. 2022. Fuzzy logic based logical query answering on knowledge graphs. In *Proceedings of the AAAI Conference on Artificial Intelligence*, Vol. 36. 3939–3948.
- [11] Nurendra Choudhary, Nikhil Rao, Sumeet Katariya, Karthik Subbian, and Chandan Reddy. 2021. Probabilistic entity representation model for reasoning over knowledge graphs. *Advances in Neural Information Processing Systems* 34 (2021), 23440–23451.
- [12] Nurendra Choudhary, Nikhil Rao, Sumeet Katariya, Karthik Subbian, and Chandan K Reddy. 2021. Self-supervised hyperboloid representations from logical queries over knowledge graphs. In *Proceedings of the Web Conference 2021*. 1373–1384.
- [13] Brian A Davey and Hilary A Priestley. 2002. *Introduction to lattices and order*. Cambridge university press.
- [14] Daniel Daza and Michael Cochez. 2020. Message passing query embedding. *arXiv preprint arXiv:2002.02406* (2020).
- [15] Tim Dettmers, Pasquale Minervini, Pontus Stenetorp, and Sebastian Riedel. 2018. Convolutional 2d knowledge graph embeddings. In *Proceedings of the AAAI conference on artificial intelligence*, Vol. 32.
- [16] Jacob Devlin, Ming-Wei Chang, Kenton Lee, and Kristina Toutanova. 2018. Bert: Pre-training of deep bidirectional transformers for language understanding. *arXiv preprint arXiv:1810.04805* (2018).
- [17] Lise Getoor and Ben Taskar. 2007. *Introduction to statistical relational learning*. MIT press.
- [18] Justin Gilmer, Samuel S Schoenholz, Patrick F Riley, Oriol Vinyals, and George E Dahl. 2017. Neural message passing for quantum chemistry. In *International conference on machine learning*. PMLR, 1263–1272.
- [19] Petr Hájek. 2013. *Metamathematics of fuzzy logic*. Vol. 4. Springer Science & Business Media.
- [20] Will Hamilton, Payal Bajaj, Marinka Zitnik, Dan Jurafsky, and Jure Leskovec. 2018. Embedding logical queries on knowledge graphs. *Advances in neural information processing systems* 31 (2018).
- [21] Ziniu Hu, Yuxiao Dong, Kuansan Wang, and Yizhou Sun. 2020. Heterogeneous graph transformer. In *Proceedings of the web conference 2020*. 2704–2710.
- [22] Shaoxiong Ji, Shirui Pan, Erik Cambria, Pekka Marttinen, and S Yu Philip. 2021. A survey on knowledge graphs: Representation, acquisition, and applications. *IEEE transactions on neural networks and learning systems* 33, 2 (2021), 494–514.
- [23] Erich Peter Klement, Radko Mesiar, and Endre Pap. 2013. *Triangular norms*. Vol. 8. Springer Science & Business Media.
- [24] Bhushan Kotnis, Carolin Lawrence, and Mathias Niepert. 2021. Answering complex queries in knowledge graphs with bidirectional sequence encoders. In *Proceedings of the AAAI Conference on Artificial Intelligence*, Vol. 35. 4968–4977.
- [25] Timothée Lacroix, Nicolas Usunier, and Guillaume Obozinski. 2018. Canonical tensor decomposition for knowledge base completion. In *International Conference on Machine Learning*. PMLR, 2863–2872.
- [26] Leonid Libkin and Cristina Sirangelo. 2009. Open and Closed World Assumptions in Data Exchange. *Description Logics* 477 (2009).
- [27] Lihui Liu, Boxin Du, Heng Ji, ChengXiang Zhai, and Hanghang Tong. 2021. Neural-answering logical queries on knowledge graphs. In *Proceedings of the 27th ACM SIGKDD conference on knowledge discovery & data mining*. 1087–1097.
- [28] Xiao Liu, Shiyu Zhao, Kai Su, Yukuo Cen, Jiezhong Qiu, Mengdi Zhang, Wei Wu, Yuxiao Dong, and Jie Tang. 2022. Mask and reason: Pre-training knowledge graph transformers for complex logical queries. In *Proceedings of the 28th ACM SIGKDD Conference on Knowledge Discovery and Data Mining*. 1120–1130.
- [29] Yinhan Liu, Myle Ott, Naman Goyal, Jingfei Du, Mandar Joshi, Danqi Chen, Omer Levy, Mike Lewis, Luke Zettlemoyer, and Veselin Stoyanov. 2019. Roberta: A robustly optimized bert pretraining approach. *arXiv preprint arXiv:1907.11692* (2019).
- [30] Ilya Loshchilov and Frank Hutter. 2019. Decoupled Weight Decay Regularization. In *International Conference on Learning Representations*. <https://openreview.net/forum?id=Bkg6RiCqY7>
- [31] Liheng Ma, Chen Lin, Derek Lim, Adriana Romero-Soriano, Puneet K. Dokania, Mark Coates, Philip H. S. Torr, and Ser-Nam Lim. 2023. Graph Inductive Biases in Transformers without Message Passing. In *International Conference on Machine Learning*. ICML 2023, 23-29 July 2023, Honolulu, Hawaii, USA (Proceedings of Machine Learning Research, Vol. 202). PMLR, 23321–23337. <https://proceedings.mlr.press/v202/ma23c.html>
- [32] Zhuang Ma and Michael Collins. 2018. Noise Contrastive Estimation and Negative Sampling for Conditional Models: Consistency and Statistical Efficiency. In *Proceedings of the 2018 Conference on Empirical Methods in Natural Language Processing*. 3698–3707.
- [33] David Marker. 2006. *Model theory: an introduction*. Vol. 217. Springer Science & Business Media.
- [34] Chau Duc Minh Nguyen, Tim French, Wei Liu, and Michael Stewart. 2023. CylE: Cylinder embeddings for multi-hop reasoning over knowledge graphs. In *Proceedings of the 17th Conference of the European Chapter of the Association for Computational Linguistics*. 1736–1751.
- [35] Maximilian Nickel, Volker Tresp, Hans-Peter Kriegel, et al. 2011. A three-way model for collective learning on multi-relational data. In *icml*, Vol. 11. 3104482–3104584.
- [36] Hongyu Ren, Hanjun Dai, Bo Dai, Xinyun Chen, Denny Zhou, Jure Leskovec, and Dale Schuurmans. 2022. Smore: Knowledge graph completion and multi-hop reasoning in massive knowledge graphs. In *Proceedings of the 28th ACM SIGKDD Conference on Knowledge Discovery and Data Mining*. 1472–1482.
- [37] Hongyu Ren, Mikhail Galkin, Michael Cochez, Zhaocheng Zhu, and Jure Leskovec. 2023. Neural graph reasoning: Complex logical query answering meets graph

- databases. *arXiv preprint arXiv:2303.14617* (2023).
- [38] Hongyu Ren*, Weihua Hu*, and Jure Leskovec. 2020. Query2box: Reasoning over Knowledge Graphs in Vector Space Using Box Embeddings. In *International Conference on Learning Representations*. <https://openreview.net/forum?id=Bjgr4kSFDS>
- [39] Hongyu Ren and Jure Leskovec. 2020. Beta embeddings for multi-hop logical reasoning in knowledge graphs. *Advances in Neural Information Processing Systems* 33 (2020), 19716–19726.
- [40] Ali Sadeghian, Mohammadreza Armandpour, Patrick Ding, and Daisy Zhe Wang. 2019. Drum: End-to-end differentiable rule mining on knowledge graphs. *Advances in Neural Information Processing Systems* 32 (2019).
- [41] Apoorv Saxena, Adrian Kochsiek, and Rainer Gemulla. 2022. Sequence-to-Sequence Knowledge Graph Completion and Question Answering. In *Proceedings of the 60th Annual Meeting of the Association for Computational Linguistics (Volume 1: Long Papers)*. 2814–2828.
- [42] Apoorv Saxena, Aditya Tripathi, and Partha Talukdar. 2020. Improving multi-hop question answering over knowledge graphs using knowledge base embeddings. In *Proceedings of the 58th annual meeting of the association for computational linguistics*. 4498–4507.
- [43] Fabian M Suchanek, Gjergji Kasneci, and Gerhard Weikum. 2007. Yago: a core of semantic knowledge. In *Proceedings of the 16th international conference on World Wide Web*. 697–706.
- [44] Zhiqing Sun, Zhi-Hong Deng, Jian-Yun Nie, and Jian Tang. 2019. RotatE: Knowledge Graph Embedding by Relational Rotation in Complex Space. In *International Conference on Learning Representations*. <https://openreview.net/forum?id=HkgEQnRqYQ>
- [45] Ilya O Tolstikhin, Neil Houlsby, Alexander Kolesnikov, Lucas Beyer, Xiaohua Zhai, Thomas Unterthiner, Jessica Yung, Andreas Steiner, Daniel Keysers, Jakob Uszkoreit, et al. 2021. Mlp-mixer: An all-mlp architecture for vision. *Advances in neural information processing systems* 34 (2021), 24261–24272.
- [46] Kristina Toutanova and Danqi Chen. 2015. Observed versus latent features for knowledge base and text inference. In *Proceedings of the 3rd workshop on continuous vector space models and their compositionality*. 57–66.
- [47] Théo Trouillon, Johannes Welbl, Sebastian Riedel, Éric Gaussier, and Guillaume Bouchard. 2016. Complex embeddings for simple link prediction. In *International conference on machine learning*. PMLR, 2071–2080.
- [48] Shikhar Vashishth, Soumya Sanyal, Vikram Nitin, and Partha Talukdar. 2020. Composition-based Multi-Relational Graph Convolutional Networks. In *International Conference on Learning Representations*. https://openreview.net/forum?id=ByLA_C4tPr
- [49] Ashish Vaswani, Noam Shazeer, Niki Parmar, Jakob Uszkoreit, Llion Jones, Aidan N Gomez, Lukasz Kaiser, and Illia Polosukhin. 2017. Attention is all you need. *Advances in neural information processing systems* 30 (2017).
- [50] Denny Vrandečić and Markus Kröttsch. 2014. Wikidata: a free collaborative knowledgebase. *Commun. ACM* 57, 10 (2014), 78–85.
- [51] B Wang, T Shen, G Long, T Zhou, Y Wang, and Y Chang. 2021. Structure-augmented text representation learning for efficient knowledge graph completion. In *Proceedings of the Web Conference 2021*. ACM.
- [52] Siyuan Wang, Zhongyu Wei, Meng Han, Zhihao Fan, Haijun Shan, Qi Zhang, and Xuanjing Huang. 2023. Query Structure Modeling for Inductive Logical Reasoning Over Knowledge Graphs. *arXiv preprint arXiv:2305.13585* (2023).
- [53] Xiaozhi Wang, Tianyu Gao, Zhaocheng Zhu, Zhengyan Zhang, Zhiyuan Liu, Juanzi Li, and Jian Tang. 2021. KEPLER: A unified model for knowledge embedding and pre-trained language representation. *Transactions of the Association for Computational Linguistics* 9 (2021), 176–194.
- [54] Xiang Wang, Tinglin Huang, Dingxian Wang, Yancheng Yuan, Zhenguang Liu, Xiangnan He, and Tat-Seng Chua. 2021. Learning intents behind interactions with knowledge graph for recommendation. In *Proceedings of the web conference 2021*. 878–887.
- [55] Zihao Wang, Weizhi Fei, Hang Yin, Yangqiu Song, Ginny Y Wong, and Simon See. 2023. Wasserstein-Fisher-Rao Embedding: Logical Query Embeddings with Local Comparison and Global Transport. *arXiv preprint arXiv:2305.04034* (2023).
- [56] Zihao Wang, Yangqiu Song, Ginny Wong, and Simon See. 2023. Logical Message Passing Networks with One-hop Inference on Atomic Formulas. In *The Eleventh International Conference on Learning Representations*. https://openreview.net/forum?id=SoyOsp71_1
- [57] Zihao Wang, Hang Yin, and Yangqiu Song. 2022. Benchmarking the Combinatorial Generalizability of Complex Query Answering on Knowledge Graphs. *Proceedings of the Neural Information Processing Systems Track on Datasets and Benchmarks 1 (NeurIPS Datasets and Benchmarks 2021)* (2022).
- [58] Chenyan Xiong, Russell Power, and Jamie Callan. 2017. Explicit semantic ranking for academic search via knowledge graph embedding. In *Proceedings of the 26th international conference on world wide web*. 1271–1279.
- [59] Wenhan Xiong, Thien Hoang, and William Yang Wang. 2017. DeepPath: A Reinforcement Learning Method for Knowledge Graph Reasoning. In *Proceedings of the 2017 Conference on Empirical Methods in Natural Language Processing*. 564–573.
- [60] Keyulu Xu, Weihua Hu, Jure Leskovec, and Stefanie Jegelka. 2019. How Powerful are Graph Neural Networks?. In *International Conference on Learning Representations*. <https://openreview.net/forum?id=ryGs6iA5Km>
- [61] Zezhong Xu, Wen Zhang, Peng Ye, Hui Chen, and Huajun Chen. 2022. Neural-symbolic entangled framework for complex query answering. *Advances in Neural Information Processing Systems* 35 (2022), 1806–1819.
- [62] Bishan Yang, Scott Wen-tau Yih, Xiaodong He, Jianfeng Gao, and Li Deng. 2015. Embedding Entities and Relations for Learning and Inference in Knowledge Bases. In *Proceedings of the International Conference on Learning Representations (ICLR) 2015*.
- [63] Dong Yang, Peijun Qing, Yang Li, Haonan Lu, and Xiaodong Lin. 2022. GammaE: Gamma Embeddings for Logical Queries on Knowledge Graphs. In *Proceedings of the 2022 Conference on Empirical Methods in Natural Language Processing*. 745–760.
- [64] Chengxuan Ying, Tianle Cai, Shengjie Luo, Shuxin Zheng, Guolin Ke, Di He, Yanming Shen, and Tie-Yan Liu. 2021. Do transformers really perform badly for graph representation? *Advances in Neural Information Processing Systems* 34 (2021), 28877–28888.
- [65] Wen Zhang, Bibek Paudel, Liang Wang, Jiaoyan Chen, Hai Zhu, Wei Zhang, Abraham Bernstein, and Huajun Chen. 2019. Iteratively learning embeddings and rules for knowledge graph reasoning. In *The world wide web conference*. 2366–2377.
- [66] Yongqi Zhang and Quanming Yao. 2022. Knowledge graph reasoning with relational digraph. In *Proceedings of the ACM web conference 2022*. 912–924.
- [67] Zhanqiu Zhang, Jie Wang, Jiajun Chen, Shuiwang Ji, and Feng Wu. 2021. Cone: Cone embeddings for multi-hop reasoning over knowledge graphs. *Advances in Neural Information Processing Systems* 34 (2021), 19172–19183.
- [68] Zhanqiu Zhang, Jie Wang, Jieping Ye, and Feng Wu. 2022. Rethinking graph convolutional networks in knowledge graph completion. In *Proceedings of the ACM Web Conference 2022*. 798–807.
- [69] Zhaocheng Zhu, Mikhail Galkin, Zuobai Zhang, and Jian Tang. 2022. Neural-symbolic models for logical queries on knowledge graphs. In *International Conference on Machine Learning*. PMLR, 27454–27478.
- [70] Zhaocheng Zhu, Zuobai Zhang, Louis-Pascal Xhonneux, and Jian Tang. 2021. Neural bellman-ford networks: A general graph neural network framework for link prediction. *Advances in Neural Information Processing Systems* 34 (2021), 29476–29490.

A MORE DETAILS ABOUT THE DATASETS

The statistics of the three knowledge graphs used in our experiment are shown in Table 6. As we described in section 5.1.1, we conduct experiments on the complex query datasets proposed in the BetaE paper [39]. The statistics for the complex queries contained in these datasets are shown in Table 1. The statistics for the answers for each query type are shown in Table 7.

As mentioned in Section 5.1.3, there are some other neural CQA models [11, 24, 28] that are trained and evaluated on the EPFO query datasets proposed in the Q2B paper [38]. To compare these models, we also conduct experiments (see Appendix C) on the FB15k-237 and NELL995 configured by the Q2B setting. We denote these two datasets as FB237-Q2B and NELL-Q2B. The statistics for the EPFO queries and corresponding answers for Q2B datasets are shown in Table 8 and Table 9.

One difference between the BetaE datasets and the Q2B datasets is the limit on the number of answers to the queries, since the Q2B datasets have queries with more than 5000 answers, almost 1/3 of some datasets. Furthermore, the Q2B datasets do not contain queries with negation. These differences mean that BetaE [39] datasets are more challenging, so most CQA models in recent years chose to evaluate their performance on the BetaE datasets. To obtain convincing comparison results, we mainly conduct experiments on the BetaE datasets to compare existing competitive neural CQA models.

Table 6: Datasets statistics, as well as training, validation and test edge splits.

Dataset	Entities	Relations	Training Edges	Validation Edges	Test Edges	Total Edges
FB15k	14,951	1,345	483,142	50,000	59,071	592,213
FB15k-237	14,505	237	272,115	17,526	20,438	310,079
NELL995	63,361	200	114,213	14,324	14,267	142,804

Table 7: The average number of answers divided by query structure.

Dataset	1p	2p	3p	2i	3i	ip	pi	2u	up	2in	3in	inp	pin	pni
FB15k	1.7	19.6	24.4	8.0	5.2	18.3	12.5	18.9	23.8	15.9	14.6	19.8	21.6	16.9
FB15k-237	1.7	17.3	24.3	6.9	4.5	17.7	10.4	19.6	24.3	16.3	13.4	19.5	21.7	18.2
NELL995	1.6	14.9	17.5	5.7	6.0	17.4	11.9	14.9	19.0	12.9	11.1	12.9	16.0	13.0

Table 8: The number of training, validation, and test queries generated for different query structures of the Q2B datasets [38].

Queries	Training		Validation		Test	
Dataset	1p	others	1p	Others	1p	Others
FB237-Q2B	149,689	149,689	20,101	5,000	22,812	5,000
NELL-Q2B	107,982	107,982	16,927	4,000	17,034	4,000

Table 9: The average number of answers divided by query structure for Q2B datasets [38].

Dataset	1p	2p	3p	2i	3i	ip	pi	2u	up
FB237-Q2B	13.3	131.4	215.3	69.0	48.9	593.8	257.7	35.6	127.7
NELL-Q2B	8.5	56.6	65.3	30.3	15.9	310.0	144.9	14.4	62.5

B MORE EXPERIMENTAL DETAILS

Our code is implemented using PyTorch. We use NVIDIA Tesla A10 GPU (24GB) and NVIDIA GeForce RTX 3090 GPU (24GB) to conduct all of our experiments. We use the AdamW [30] optimizer, whose weight decay is $1e-4$, to tune the parameters. The learning rate is $5e-5$ for NELL995 and FB15k-237 and $1e-4$ for FB15k. The batch size is 512 for NELL995 and FB15k-237 and 1,024 for FB15k. The training epoch for all datasets is 100. Following CQD-CO [3] and LMPNN [56], we choose ComplEx-N3 [25, 47] as the neural link predictor for fair comparison. In this case, we consider the logical message encoding function ρ corresponding to Equations 10–13. For these equations, the λ is a hyperparameter that needs to be determined. In LMPNN application, for simplicity, LMPNN just lets $3\lambda \|\cdot\| = 1$ and then all denominators in these closed-form expressions are 1, namely:

$$\rho(t, r, t \rightarrow h, 0) := \bar{r} \otimes t, \quad (20)$$

$$\rho(h, r, h \rightarrow t, 0) := r \otimes h, \quad (21)$$

$$\rho(t, r, t \rightarrow h, 1) := -\bar{r} \otimes t, \quad (22)$$

$$\rho(h, r, h \rightarrow t, 1) := -r \otimes h. \quad (23)$$

To make a fair comparison with LMPNN, in CLMPT application, we also use the logical message encoding function ρ defined in Equations 20–23 to compute messages passed to the variable nodes. For the experiments (see Section 5.3.1) to evaluate how much unnecessary computational costs can be avoided by conditional logical message passing mechanism, we repeat the experiments three times on an RTX 3090 GPU and then average the calculated \downarrow Memory (see Equation 18) and \downarrow Time (see Equation 19) metrics.

C COMPARISON WITH MORE NEURAL CQA MODELS ON Q2B DATASETS

To further evaluate the performance of CLMPT, we also consider comparing neural CQA models that cannot handle logical negation and are trained and evaluated on Q2B datasets, including GQE [20], Q2B [38], BIQE [24], PERM [11], kgTransformer [28], and SILR [52]. Among these models, BIQE, kgTransformer, and SILR all use the transformer [49] to encode complex queries directly. BIQE and SILR serialize the query graph and treat the CQA task as the sequence learning task to solve. kgTransformer uses the pre-training and fine-tuning strategies based on Heterogeneous Graph Transformer (HGT) [21] to answer complex queries. In essence, kgTransformer is also a transformer-based graph neural network. We use the results

Table 10: The Hits@3 results of other neural CQA baselines on answering EPFO queries generated by Q2B [38]. Avg_p represents the average results of these EPFO query types. The boldface indicates the best results.

Dataset	Model	1p	2p	3p	2i	3i	pi	ip	2u	up	Avg _p
FB237-Q2B	GQE	40.5	21.3	15.3	29.8	41.1	18.2	8.5	16.7	16.0	23.0
	Q2B	46.7	24.0	18.6	32.4	45.3	20.5	10.8	23.9	19.3	26.8
	BIQE	47.2	29.3	24.5	34.5	47.3	21.1	9.6	7.5	14.5	26.2
	PERM	52.0	28.6	21.6	36.1	49.0	21.2	12.8	30.5	23.9	30.6
	kgTransformer	45.9	31.2	27.6	39.8	52.8	28.6	18.9	26.3	21.4	32.5
	SILR	47.1	30.2	24.9	35.8	48.4	22.2	11.3	28.3	18.1	29.6
	CLMPT	50.5	31.3	26.7	39.0	52.1	27.7	16.3	28.6	24.1	32.9
NELL-Q2B	GQE	41.7	23.1	20.3	31.8	45.4	18.8	8.1	20.0	13.9	24.8
	Q2B	55.5	26.6	23.3	34.3	48.0	21.2	13.2	36.9	16.3	30.6
	BIQE	63.2	31.0	33.2	37.0	52.5	16.4	9.1	17.3	18.4	30.9
	PERM	58.1	28.6	24.3	35.2	50.8	19.5	14.3	46.0	20.0	32.8
	kgTransformer	62.5	40.1	36.7	40.5	54.6	30.6	20.3	46.9	27.0	39.9
	SILR	64.1	32.9	33.7	37.6	53.2	17.7	5.5	45.0	18.0	34.2
	CLMPT	64.3	39.9	36.5	42.1	54.1	28.1	22.1	48.9	33.4	41.1

reported in these papers [28, 52] for comparison. Since they report the Hits@3 results, for a fair comparison, we also use Hits@3 as the evaluation metric, which calculates the proportion of correct answer entities ranked among the top 3.

As shown in the results in Table 10, CLMPT reaches the best performance on average across all datasets. For those models that use the transformer to encode the entire query graph directly, namely BIQE, SILR, and kgTransformer, we speculate that their insufficient graph inductive biases may negatively affect their performance. To encode the entire query graph at once using the transformer, BIQE designs a special positional encoding scheme, and SILR designs a particular graph serialization method and structural prompt. These designs can be viewed as introducing specific graph inductive biases into the transformer to encode the query graph. For kgTransformer, it relies primarily on the graph inductive biases of the HGT architecture. According to the progress of the graph transformers [31, 64], graph inductive biases are critical to using the transformer to encode graph data. In particular, structural encoding is important for the graph transformers without message passing. Therefore, we speculate that the graph inductive biases introduced by these CQA models may not be sufficient to encode the query graph that defines complex logical dependencies. On the other hand, it is not clear how to introduce appropriate graph inductive biases for query graphs that define first-order logical dependencies. By contrast, CLMPT, based on logical message passing, uses the transformer to aggregate messages and update node embeddings rather than to encode the entire query graph. This difference makes CLMPT less dependent on graph inductive biases than the transformer-based CQA models mentioned above. However, it also suggests that appropriate graph inductive biases may enhance the performance of CLMPT. This extension can be explored in the future.

D ANALYSES ON MODEL PARAMETERS

Since CLMPT introduces the transformer, it has more parameters than LMPNN. To further evaluate the effectiveness of CLMPT, we compare LMPNN using a smaller model whose parameters are close to those of LMPNN. Specifically, we set TE layer = 1 and

$d_{FFN} = 4096$, and we represent such a smaller model as CLMPT-small. Since the parameters of the neural link predictor in LMPNN are frozen, we consider using both frozen and trainable neural link predictors for fair comparison. We represent the models in these two cases as CLMPT-small(F) and CLMPT-small(T), respectively. The experimental results are shown in Table 11. When their model parameters are close, CLMPT still achieves the best average performance on EPFO queries. In the case of freezing the neural link predictor, CLMPT-small(F) has fewer trainable parameters than LMPNN on NELL995, but it still significantly outperforms LMPNN on average in answering EPFO queries. These experimental results reflect the effectiveness of CLMPT.

E COMPARISON WITH SYMBOLIC INTEGRATION MODELS

We discuss the differences between symbolic integration CQA models and neural CQA models in Section 2. The model proposed in this paper is a neural CQA model, so our comparisons and related discussions are mainly carried out within the scope of neural CQA models. Since symbolic information can enhance the performance of neural CQA models [56], in this section, we consider two representative symbolic integration models, GNN-QE [69] and ENeSy [61], for comparison with CLMPT to show the potential. We list the MRR results reported in their original papers. The results are shown in Table 12. It is found that CLMPT is also competitive even with the symbolic integration models on answering EPFO queries. Specifically, CLMPT achieves a better average performance than these symbolic integration models on EPFO queries for NELL995. For FB15k-237, CLMPT still has a gap in performance with GNN-QE, but it can outperform ENeSy on EPFO queries. For the negative queries, there are still gaps between the neural CQA models and these symbolic integration models because the fuzzy sets equipped with symbolic information used in the reasoning process of these models can effectively deal with logical negation through probabilistic values. These results suggest that neural models can be potentially improved with symbolic integration. However, it is worth

Table 11: The MRR results of CLMPT-small using frozen neural link predictor and using trainable neural link predictor. Param_T and Param_F represent trainable and frozen parameters of the model, respectively. The F in parentheses indicates that the model uses a frozen neural link predictor, and T indicates that it uses a trainable one.

Dataset	Model	1p	2p	3p	2i	3i	pi	ip	2u	up	2in	3in	inp	pin	pni	Avg _p	Avg _n	Param _T	Param _F
FB15k-237	LMPNN	45.9	13.1	10.3	34.8	48.9	22.7	17.6	13.5	10.3	8.7	12.9	7.7	4.6	5.2	24.1	7.8	16M	30M
	CLMPT-small(F)	46.1	12.6	10.0	36.1	50.4	26.7	17.5	14.9	10.3	7.7	11.6	7.5	4.4	5.0	25.0	7.3	32M	30M
	CLMPT-small(T)	45.7	13.2	11.0	37.2	51.6	27.4	18.2	14.3	11.1	7.4	13.1	8.1	5.1	4.7	25.5	7.7	62M	0M
NELL995	LMPNN	60.6	22.1	17.5	40.1	50.3	28.4	24.9	17.2	15.7	8.5	10.8	12.2	3.9	4.8	30.7	8.0	33M	128M
	CLMPT-small(F)	60.6	21.7	17.7	42.2	51.7	30.7	24.5	19.4	15.6	6.4	7.9	11.0	3.7	4.5	31.6	6.7	32M	128M
	CLMPT-small(T)	59.1	21.3	17.5	41.8	51.8	29.0	23.5	19.0	15.6	6.4	7.9	11.2	3.8	4.5	31.0	6.8	160M	0M

Table 12: The MRR results of symbolic integration models and CLMPT. The boldface indicates the best results.

Dataset	Model	1p	2p	3p	2i	3i	pi	ip	2u	up	2in	3in	inp	pin	pni	Avg _p	Avg _n
FB15k-237	GNN-QE	42.8	14.7	11.8	38.3	54.1	31.1	18.9	16.2	13.4	10.0	16.8	9.3	7.2	7.8	26.8	10.2
	ENeSy	44.7	11.7	8.6	34.8	50.4	27.6	19.7	14.2	8.4	10.1	10.4	7.6	6.1	8.1	24.5	8.5
	CLMPT-small(F)	46.1	12.6	10.0	36.1	50.4	26.7	17.5	14.9	10.3	7.7	11.6	7.5	4.4	5.0	25.0	7.3
	CLMPT	45.7	13.7	11.3	37.4	52.0	28.2	19.0	14.3	11.1	7.7	13.7	8.0	5.0	5.1	25.9	7.9
NELL995	GNN-QE	53.3	18.9	14.9	42.4	52.5	30.8	18.9	15.9	12.6	9.9	14.6	11.4	6.3	6.3	28.9	9.7
	ENeSy	59.0	18.0	14.0	39.6	49.8	29.8	24.8	16.4	13.1	11.3	8.5	11.6	8.6	8.8	29.4	9.8
	CLMPT-small(F)	60.6	21.7	17.7	42.2	51.7	30.7	24.5	19.4	15.6	6.4	7.9	11.0	3.7	4.5	31.6	6.7
	CLMPT	58.9	22.1	18.4	41.8	51.9	28.8	24.4	18.6	16.2	6.6	8.1	11.8	3.8	4.5	31.3	7.0

noting that introducing additional symbolic information requires larger computational costs.

According to [37, 56], for larger knowledge graphs, neural CQA models and symbolic integration models have different scalabilities. As we discussed in Section 2, symbolic integration models require more computing resources and are more likely to suffer from scalability issues. For example, GNN-QE employs NBFNet [70] to compute message passing on the whole KG, resulting in complexity that is linear to $(|\mathcal{E}| + |\mathcal{V}|)d$, where $|\mathcal{E}|$ is the number of edges in KG, $|\mathcal{V}|$ is the number of nodes in KG, and d is the embedding dimension. For CLMPT, which only performs message passing on the query graph, the complexity is just $O(d)$. Besides, GNN-QE estimates the probability of whether each entity is the answer at each

intermediate step, making the size of its fuzzy sets scale linearly with $|\mathcal{V}|$. As a result, GNN-QE requires much more computational costs, requiring 128GB GPU memory to run a batch size of 32. For CLMPT-small(F), which has only 32M trainable parameters, it only requires less than 12GB GPU memory to run a batch size of 1024. Even in this case, CLMPT-small(F) can still achieve performance competitive with GNN-QE on NELL995.

We suspect that integrating symbolic information into CLMPT can improve the performance, especially on negative queries. However, exploring how to integrate symbolic information into CLMPT is beyond the scope of this paper. This extension is left for future work.